J Membrane Biol (2013) 246:263–269
DOI 10.1007/s00232-013-9527-x

ORIGINAL ARTICLES

Diffusion Behaviors of Fluorescence Probe Molecules Through the Stratum Corneum Layer Under Physical Stress

Ho Lee · Jin Woong Kim

Received: 12 November 2012 / Accepted: 15 January 2013 / Published online: 31 January 2013

Abstract This study experimentally demonstrates how application of an external physical stress onto the skin membrane affects the permeation of penetrating molecules. As a proxy of active compounds, in this study, a series of fluorescence probe molecules were utilized. We observed that skin permeation could be enhanced by imparting vertical strokes from a tapping head consisting of projections onto the skin. This was confirmed with consistency from in vitro and in vivo transdermal permeation studies. After an effective physical stress was applied to the skin, the permeation depth of probe molecules remarkably increased, which was comparable to the case of topical treatment. This seems to arise from temporal disordering of the stratum corneum layer in response to the applied physical stress.

Keywords Physical stress · Skin permeability · Projection · Stratum corneum

Introduction

A key function of the stratum corneum, the outermost layer of the skin, is to block any penetration of invaders. Because of this unique function, topical administration of drug molecules is often limited or not effective (Elias 2005; Michaels et al. 1975). In an attempt to enhance drug-delivery efficiency through the skin, advances in the development of novel technologies, including chemical enhancement, iontophoresis, electroporation, sonophoresis and microneedling, have been made (Prausnitz et al. 2004; Brown et al. 2006; Kalia et al. 2004; Doukas and Kollias 2004; Lavon and Kost 2004; Prausnitz 2004; Mitragotri 2006). Use of chemical enhancers, indeed, helps drug molecule transport through the skin; however, only small drug molecules are available since the diffusivity of penetrating molecules depends on their molecular weight. Using an electric field or acoustic energy, more enhanced drug delivery can be achieved. However, complicated equipment is basically required for these approaches. Alternatively, microneedling techniques that pierce the skin to form microchannels can be used; in the aspect of aesthetic applications, skin safety often becomes an issue.

The skin likely changes its physical or biological properties in response to the physical stress applied. Physical stresses include pressure, tension, motion, vibration and so on. A good example can be found in the massage process. External physical stress is continuously applied to the human skin and/or body and has been known to show physiological and therapeutic efficacy; it is indeed useful for relieving pain and soothing the nervous system as well as for accelerating the elimination of tissue waste and increasing the absorption of nutrients (Eccles and Aberd 1896; Mortimer et al. 1990). In particular, it has been generally accepted, in terms of topical treatment as well as delivery systems, that application of physical stress onto the skin enhances the absorption of dermatologically active compounds. However, only a few studies have been performed to confirm the effect of applying external physical stress on enhancing transdermal delivery efficiency (Sakurai et al. 2005; Treffel et al. 1993). From the standpoint of exploring more improved transdermal

H. Lee
School of Mechanical Engineering, Kyungpook National University, Daegu 702-701, Korea

J. W. Kim (✉)
Department of Applied Chemistry, Hanyang University, Ansan, Gyeonggi-do 426-791, Korea
e-mail: kjwoong@hanyang.ac.kr

delivery techniques, therefore, a more systematic understanding of how application of physical stress on the skin affects the permeability of penetrating molecules is needed.

Here, as a proof of concept, we investigated the effect of external physical stress on improving the skin permeation of penetrating molecules. For this, a demonstration experimental setup, in which a tapping force was mechanically imparted to skin samples, was prepared. The key of our approach was to give vertical strokes onto the skin from topologically tapping heads. A flat disk and a disk with tiny projections were employed in this study. Then, the permeation of probe molecules through the test skins was characterized in vitro and in vivo using confocal laser scanning microscope (CLSM) techniques.

Experimental Methods

Materials

Nile red, propylene glycol and phosphate-buffered saline (pH 7.4) tablets were purchased from Sigma-Aldrich (St. Louis, MO). Lucifer yellow CH lithium salt and dextran–tetramethylrhodamine (3×10^3 and 1×10^4 g/mol) were purchased from Invitrogen (Carlsbad, CA). Methanol was of HPLC grade and purchased from J. T. Baker (Phillipsburg, NJ). Hartley albino guinea pigs for in vitro and in vivo experiments were purchased from Orient (Wenzhou, China).

Setting Up a Customized Tapping Force Generator

Dorsal skins of full thickness were excised from Hartley albino guinea pigs. Then, they were pretreated using the tapping disks. One was a flat silicone disk with 15 mm diameter (flat type). The other was a silicone disk with 36 projections on the bottom (projection type). The diameter and height projections were 1 and 1.5 mm, respectively. Nile red (0.01 wt%) dissolved in propylene glycol was evenly spread on the skin using a roller, and then the skin was mounted on the customized device (see Fig. 1). In order to monitor the tapping force, we employed a film-type piezoelectric force sensor (FlexiForce Sensor A201; Tekscan, Boston, MA), which uses resistance-based technology. The application of a force to the active sensing area of the sensor results in a change in the resistance of the sensing element in inverse proportion to the force applied. The applied force can then be measured by monitoring the change in resistance of the sensing element. The tapping force in our experiment was set to 1 N, and the tapping was carried out 50 times ($n = 4$ for each testing group). As controls, one group of samples was topically treated with Nile red only.

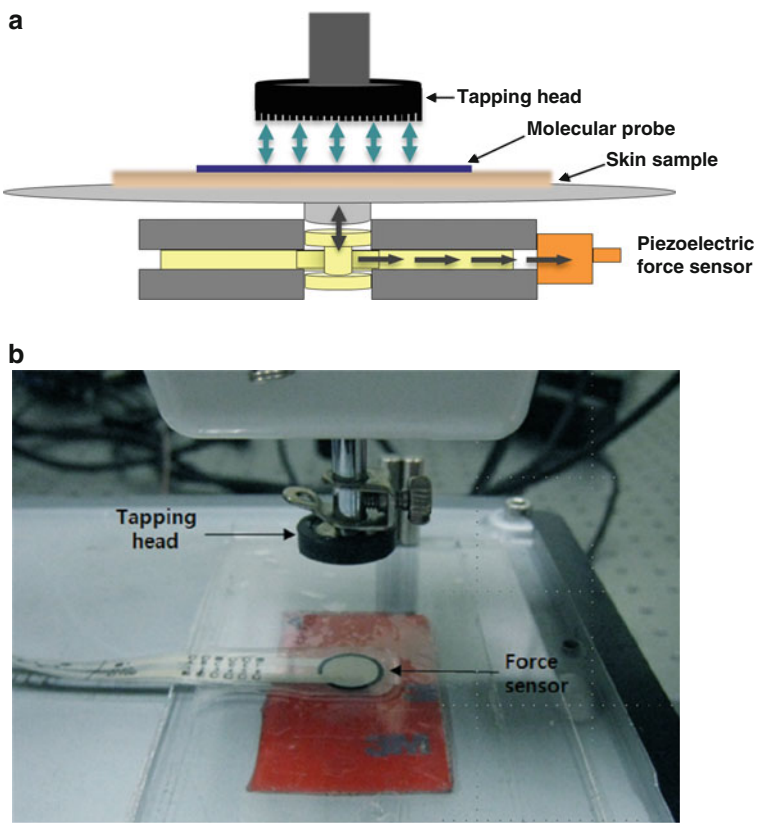

Fig. 1 A customized tapping force generator

Imaging of In Vitro Penetration Profiles

Penetration profiles of fluorescence probes were imaged using CLSM. The penetration depth of fluorescence probes was obtained by taking the florescence intensity along the z direction of cross-sectioned skin samples. A laser diode-pumped Ti:sapphire laser was employed as a light source. The wavelength was selected based on the excitation peak of Nile red. The laser power on the sample was adjusted using a series of optical attenuators. A water-immersing objective lens (C Apochromat ×40; Zeiss, Oberkochen, Germany) with a numerical aperture of 1.2 and a working distance of 170 μm was used. The microscope was built as an inversion type. The microscopic view area was set to 300 × 300 μm. The z axis scanning used a motorized scanner. The optical sectioning thickness was approximately 4 μm. The signals from both photomultiplier tubes were fed into an A/D convertor, and digitally converted signals were used to produce a snapshot image.

In Vivo Transdermal Permeation Study

Three types of fluorescence probes were used for the in vivo permeation study: Nile red (a lipophilic probe), lucifer yellow (a hydrophilic–ionic probe) and Texas red-labeled dextran polymers (a hydrophilic–neutral probe). These probe molecules were dissolved in propylene glycol or deionized water with 0.01 wt% concentration. In this observation, the tapping head consisted of 36 bundles of polybutylene terephthalate (PBT) fibers. The thickness of each fiber was approximately 30 μm. The head area was 2.5 × 0.8 cm, and each bundle had approximately 50 PBT fibers. First, a 0.05-ml probe solution was topically applied to the testing skin. The dorsal area of 6-week-old Hartley albino guinea pigs was used. Then, the skin was tapped 50 times by an applied force of 1 N. One hour later, full-thickness skin was biopsied with an 8-mm biopsy punch. The disk-shaped biopsies were cross-sectioned with a cryostat microtome. Localization of fluorescence in the guinea pig skin was examined using a Zeiss LSM 510 confocal microscope. All confocal images were acquired in the same setting parameters. Analyzed data from confocal images represent the mean values and standard deviation ($n \geq 20$). Statistical analysis was conducted using the Mann–Whitney test, and significant differences were accepted when $p < 0.05$.

Results

A flat disk head and a disk with tiny projections on the bottom were used in this study. The vertical tapping force applied to each disk was 1 N. The flat disk head with 15 mm diameter produces 6.5 kPa. The disk with projections made for this study also has the same head dimension but consists of 36 projections on the head surface. The diameter of each projection is 1 mm. Hence, each projection produces ∼28 mN and ∼35.7 kPa. The pressure produced from the projection head is higher than that from the flat head by a factor of 5. As controls, simple topical treatment was considered. In this case, the skin was topically treated with probe molecules only.

To determine the penetration depth of probe molecules in the skin, Nile red was diffused after application of physical stress on the skin. The location of Nile red in the skin was imaged using CLSM (Fig. 2a–c). Analysis of optical z-section profiles obtained from CLSM showed that after physical treatment with the disk with projections, Nile red diffused into deeper skin. The diffusion depth was comparable to the cases after flat disk treatment and topical treatment. No damage of the skin structure or corneocyte cell structure was observed after application of the tapping force to the skin, as shown in Fig. 2a–c. The average absorption area of Nile red was calculated from z-section profiles ($n > 7$, Fig. 2d). The vertical tapping stress generated from the projection-type head was indeed effective for enhancing the skin permeation of Nile red.

More studies were carried out to further investigate the effect of molecular properties of probe molecules. Molecular weight and lipophilicity were selected as the key variables in this study. The locations of fluorescence dyes in the skin were imaged using CLSM after in vivo transdermal delivery. While delivering the dyes into the model guinea pig skin, the designed tapping forces were applied for the given period of time. After topical treatment, the lipophilic fluorescence dye Nile red was detected only in the stratum corneum layer (Fig. 3a). By contrast, Nile red could be detected to a depth of 50–70 μm, when the tapping stress from the projection-type head was applied (Fig. 3b). When using the hydrophilic–ionic fluorescence dye lucifer yellow, there was no significant difference in the penetration depth between the treatment methods (Fig. 3c, d) except that some partitioning through hair follicles was detected. The penetration of hydrophilic–neutral polymer, dextran-labeled with Texas red, was also observed after physical treatments (Fig. 4). Even though the molecular weight was high, dextran molecules could be distributed to a maximum of 50 μm.

Fluorescence intensity as a function of skin depth was analyzed from the CLSM images in Figs. 3 and 4. Then, the average penetration depths were determined. Penetration depth was defined as the length scale in which fluorescence signals could be detected. As shown in Fig. 5a, the penetration depth of Nile red and dextran polymers (Dx 3000 and Dx 10000) with 3.0×10^3 and 1.0×10^4 g/mol after tapping treatment with the projection-type head were

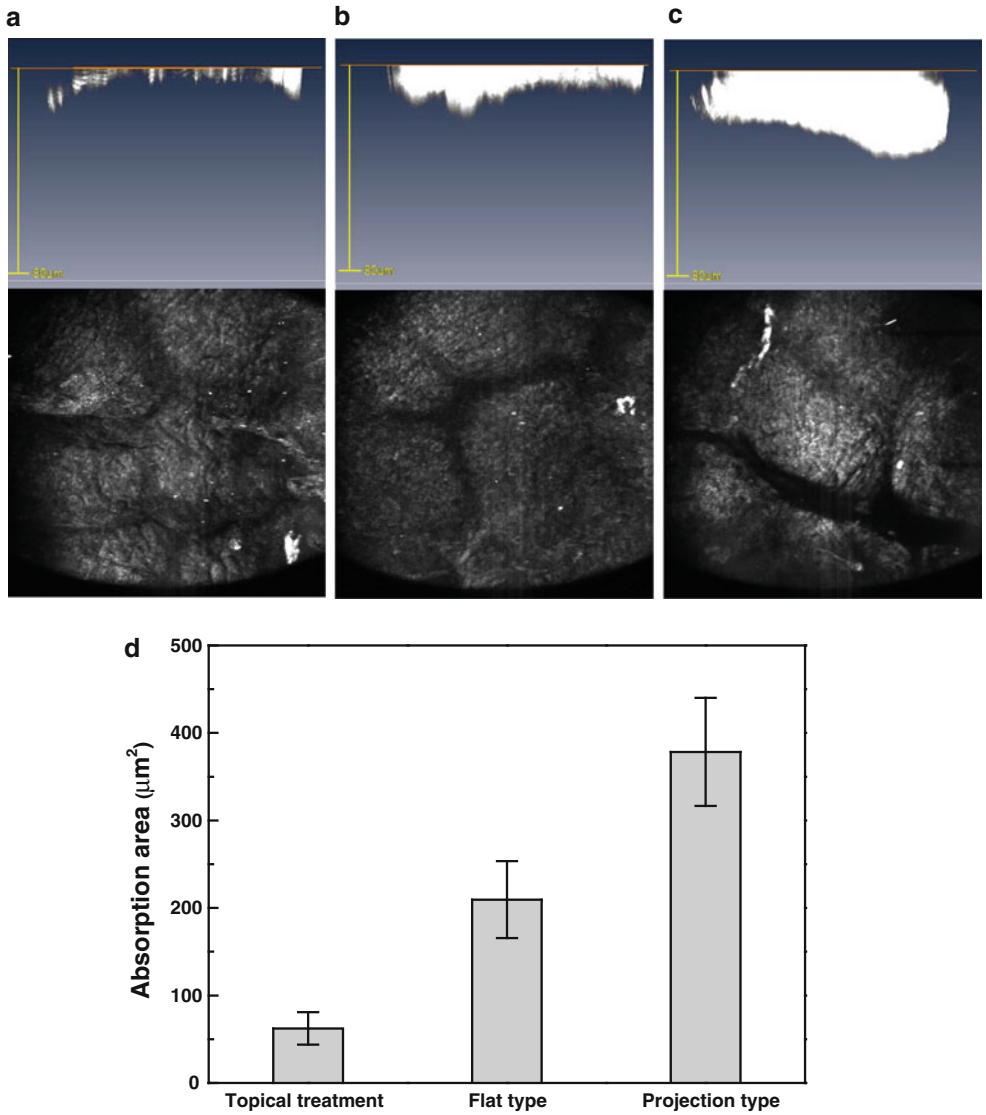

Fig. 2 Optical *z*-section fluorescence profiles of skin samples. Fluorescence intensity of *Nile red* diffused into the skin was imaged. **a** Topical treatment, **b** flat-type head treatment and **c** projection-type head treatment. **d** Average absorption areas of *Nile red* calculated from *z*-section profiles (Color figure online)

increased by 3, 1.6 and 1.4 times, respectively. Also, the penetration depth as a function of the molecular weight of penetrants is shown in Fig. 5b. Except for the case of using ionic penetrants, the penetration depth of lipophilic and neutral penetrants regressed as their molecular weights increased.

Discussion

From in vitro and in vivo skin permeation studies, we observed that application of a physical stress onto the skin significantly enhances the skin permeability. Especially, our study shows that the geometry of the tapping head essentially affects the skin permeability. The projection head with a smaller contact area provides a stronger pressure to the skin compared with the flat head. Karande and Mitragotri (2003) reported that a bundle of small reservoirs is more effective for permeation of molecules across the skin than a large single reservoir having the same area. They asserted that more enhanced permeation can be obtained by modifying the reservoir geometry rather than by changing the formulation. Similarly, Mikszta et al. (2002) also reported that use of microenhancer array devices mechanically lowers the skin barrier. Mechanical approaches have been developed to lower the skin barrier function. They include ultrasound, pressure wave, electric field, jet injection, and needling. In principle, application of a physical wave, such as ultrasound, pressure wave, and electric field, is known to generate putative pores in the

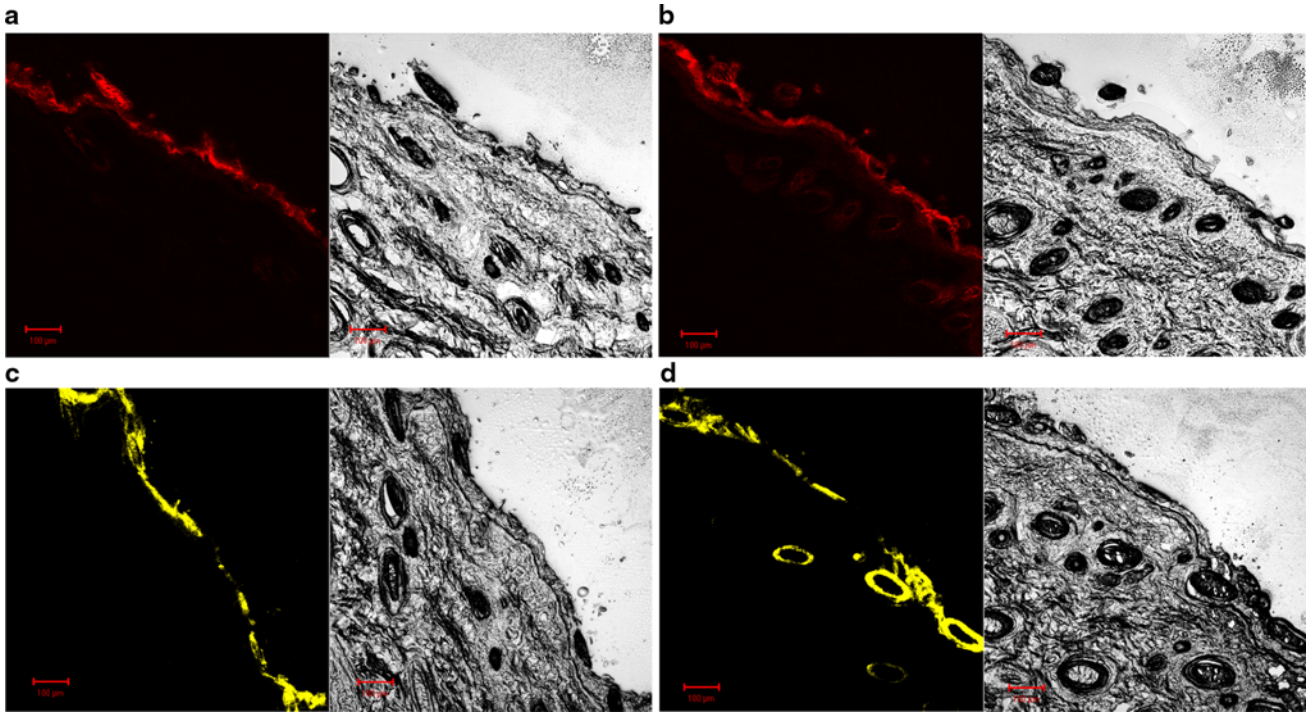

Fig. 3 CLSM images of vertically cross-sectioned skins. **a** Topical treatment with *Nile red*. **b** *Nile red* treatment with a projection-type head. **c** Topical treatment with *lucifer yellow*. **d** *Lucifer yellow* treatment with a projection-type head (Color figure online)

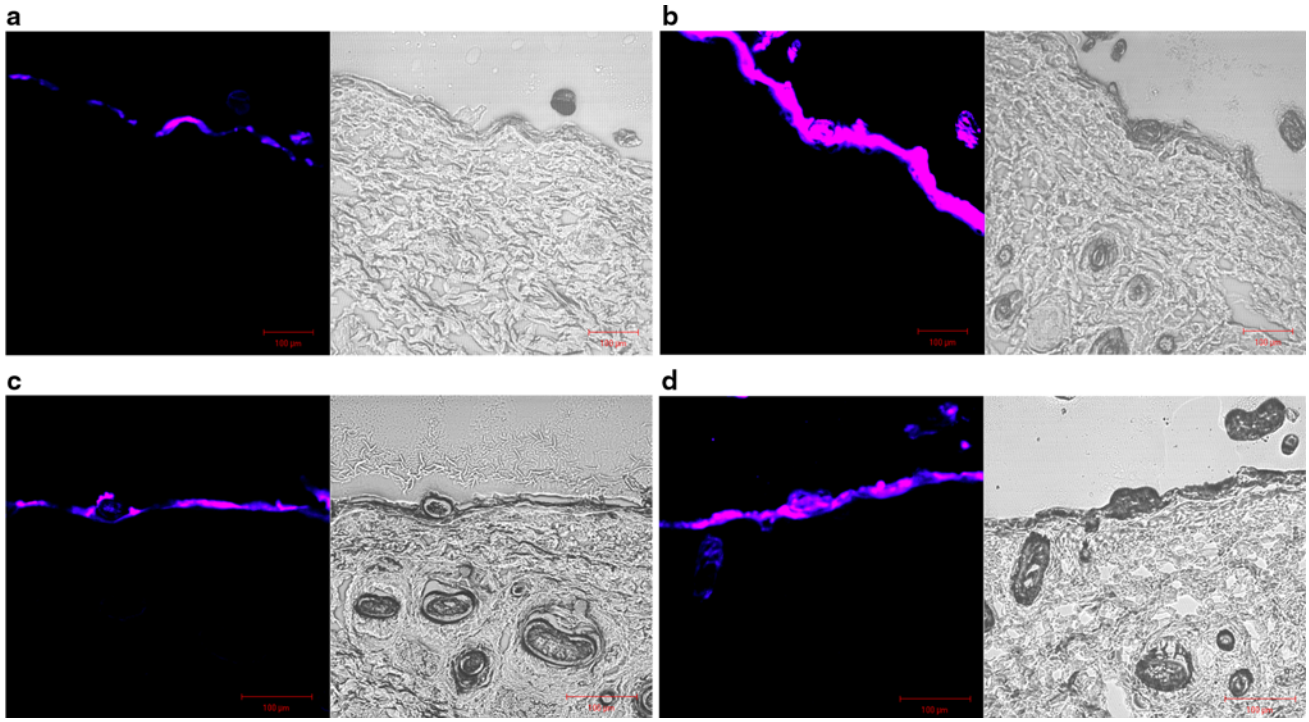

Fig. 4 CLSM images of vertically cross-sectioned skins. **a** Topical treatment of *Texas red*-labeled dextran (3.0×10^3 g/mol). **b** *Texas red*-labeled dextran (3.0×10^3 g/mol) treatment with a projection-type head. **c** Topical treatment of *Texas red*-labeled dextran (1.0×10^4 g/mol). **d** *Texas red*-labeled dextran (1.0×10^4 g/mol) treatment with a projection-type head (Color figure online)

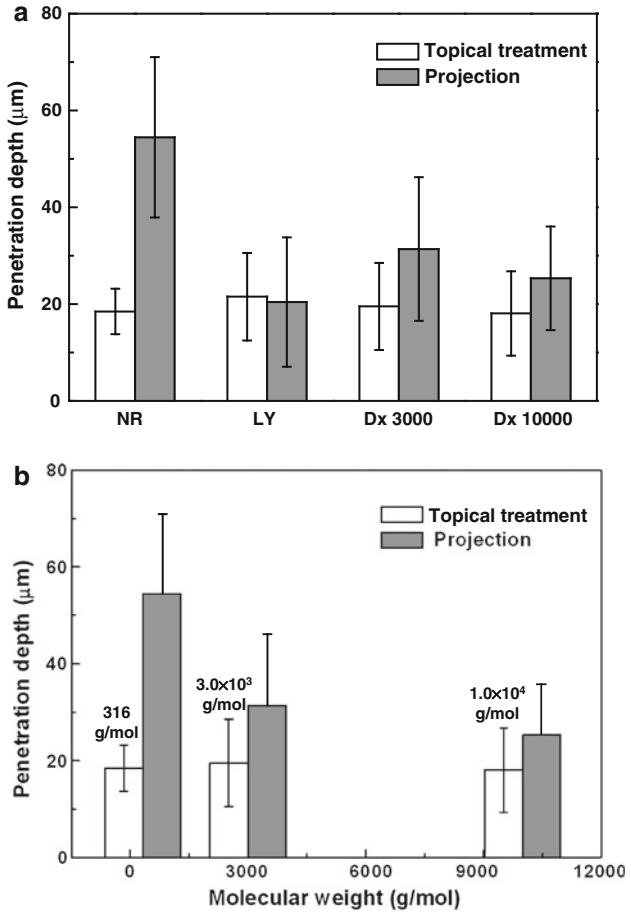

Fig. 5 **a** Average penetration depth of each fluorescence probe in guinea pig skin after consecutive treatments with a projection-type head for 5 days. *NR* Nile red, *LY* lucifer yellow, *Dx 3000* dextran of 3.0×10^3 g/mol, *Dx 10000* dextran of 1.0×10^4 g/mol. **b** Average penetration depth of fluorescence probe molecules with their molecular weight

stratum corneum layer. The pores are generated as the wave targets the weaker intercellular lipid lamellae phase rather than the tough corneocytes. Jet injection and microneedling also make holes of a diameter <100 μm. Although the working mechanisms are different, they commonly produce microchannels through the skin. Based on this, it is likely that our projection treatment also generated putative micropores in the skin. Therefore, drug molecules even with high molecular weights could diffuse through them, as shown in Figs. 4 and 5b.

To achieve an effective transdermal delivery, a typical operation pressure should be applied for a specific time; e.g., a pressure wave needs 30–100 MPa for 100–10 μs and ultrasound needs 0.1–0.5 MPa for tens of minutes. Baxter and Mitragotri (2005) proposed a theoretical model for prediction of the hole depth as a function of jetting stress. This model correlates a critical stress for skin disruption with Young's modulus of the skin. The critical stress ranges 0.46–5.8 MPa. Pedersen and Jemec (2006) also reported that mechanical stress generated from a suction cup device enhances skin permeability. A breaking threshold for the mechanical integrity of the human stratum corneum is 20–40 kPa (Treffel et al. 1993; Raphael et al. 2001). A passive transport of molecules occurs through the defects generated in the intercellular lipid matrix of the stratum corneum. The probability of forming defects is $\frac{P_{\mathrm{def}}}{P_{\mathrm{bl}}} = \exp(-\frac{\Delta G_{\mathrm{def}}}{k_{\mathrm{B}}T})$, where P_{def} is the probability for given molecules to exist as a defect and P_{bl} is the probability for the molecules to be in the lipid matrix. This indicates that the rate of lateral movement of molecules depends on the possibility of forming defects (Evans and Yeung 1994; Pedersen and Jemec 2006). The experimental results obtained in this study show that effective generation of pressure from the projections leads to temporal formation of defects in the skin.

Skin permeability also depends on the lipophilicity of penetrants. This can be estimated by the octanol–water partition coefficient, K_{OW}, and the molecular size of permeating molecules (Mitragotri 2003). The K_{OW} of Nile red is 3.10, implying that skin permeability primarily depends on free volume diffusion through the lipid matrix (Borgia 2005). Texas red-conjugated dextran molecules are assumed to be moderately hydrophilic because the maximum solubility of dextran conjugates in water is $\sim$100 mg/ml ($0.01 < K_{\mathrm{OW}} < 1$). In terms of the K_{OW} value, their skin permeation should be characterized not by considering how many aqueous pores or shunts are present but by analyzing how many penetrants pass through the lipid matrix. This indicates that when the physical stress is continuously applied to the skin, diffusion of penetrants through the lipid matrix would be enhanced. However, in the case of diffusing lucifer yellow, which is a highly hydrophilic solute with a K_{OW} of -6.846, the main permeation should be through aqueous pores and/or shunts (Chan et al. 2005). Thus, the fluorescence signal of lucifer yellow is intense in the outermost layer of the stratum corneum, hair follicles, and sweat ducts. Their surface areas are so small in the skin that the skin permeability of lucifer yellow was not significant even after physical treatments.

Conclusions

This study has experimentally demonstrated that application of an effective physical stress onto the skin significantly enhanced the skin permeability of penetrating molecules. Using a tapping head with a bundle of tiny projections, a more effective physical stress could be delivered to the skin. Our physical approach to treat the skin by means of projections led to a remarkable increase in the diffusion of penetrants. This is closely related to the

change in matrix property of the stratum corneum. The mechanical stress applied from a tapping head with a bundle of projections may reduce the viscosity resistance of the stratum corneum layer, which makes trans-layer flux of penetrants more favorable. We expect that the results obtained from this study can be used to increase the delivery efficiency of drug molecules for applications in transdermal delivery.

Acknowledgments This work was supported by the research fund of Hanyang University (HY-2011-N). This work is also supported by the National Research Foundation (NRF) Grant funded by the Korean Government (MEST) (2011-0014663).

References

Baxter J, Mitragotri S (2005) Jet-induced skin puncture and its impact on needle-free jet injections: experimental studies and a predictive model. J Control Release 106:361–373

Borgia SL (2005) Lipid nanoparticles for skin penetration enhancement—correlation to drug localization within the particle matrix as determined by fluorescence and parelectric spectroscopy. J Control Release 110:151–163

Brown MB, Martin GP, Jones SA, Akomeah FK (2006) Dermal and transdermal drug delivery systems: current and future prospects. Drug Deliv 13:175–187

Chan ECY, Tan WL, Ho PC, Fang LJ (2005) Modeling Caco-2 permeability of drugs using immobilized artificial membrane chromatography and physicochemical descriptors. J Chromatogr A 1072:159–168

Doukas AG, Kollias N (2004) Transdermal drug delivery with a pressure wave. Adv Drug Deliv Rev 56:559–579

Eccles AS, Aberd MB (1896) The practice of massage. Nature 54: 411–412

Elias PM (2005) Stratum corneum defensive functions: an integrated view. J Investig Dermatol 125:183–200

Evans E, Yeung A (1994) Hidden dynamics in rapid changes of bilayer shape. Chem Phys Lipids 73:39–56

Kalia YN, Naik A, Garrison J, Guy RH (2004) Iontophoretic drug delivery. Adv Drug Deliv Rev 56:619–658

Karande P, Mitragotri S (2003) Dependence of skin permeability on contact area. Pharm Res 20:257–263

Lavon I, Kost J (2004) Ultrasound and transdermal drug delivery. Drug Discov Today 9:670–676

Michaels AS, Chandrasekaran SK, Shaw JE (1975) Drug permeation through human skin: theory and in vitro experimental measurement. AlChE J 21:985–996

Mikszta JA, Alarcon JB, Brittingham JM, Sutter DE, Pettis RJ, Harvey NG (2002) Improved genetic immunization via micromechanical disruption of skin-barrier function and targeted epidermal delivery. Nat Med 8:415–419

Mitragotri S (2003) Modeling skin permeability to hydrophilic and hydrophobic solutes based on four permeation pathways. J Control Release 86:69–92

Mitragotri S (2006) Current status and future prospects of needle-free liquid jet injectors. Nat Rev Drug Discov 5:543–548

Mortimer PS, Simmonds R, Rezvani M, Robbins M, Hopewell JW, Ryan TJ (1990) The measurement of skin lymph flow by isotope clearance—reliability, reproducibility, injection dynamics, and the effect of massage. J Investig Dermatol 95:677–682

Pedersen L, Jemec GBE (2006) Mechanical properties and barrier function of healthy human skin. Acta Derm Venereol 86:308–311

Prausnitz MR (2004) Microneedles for transdermal drug delivery. Adv Drug Deliv Rev 56:581–587

Prausnitz MR, Mitragotri S, Langer R (2004) Current status and future potential of transdermal drug delivery. Nat Rev Drug Discov 2:115–124

Raphael RM, Waugh RE, Svetina S, Zeks B (2001) Fractional occurrence of defects in membranes and mechanically driven interleaflet phospholipid transport. Phys Rev E 64:051913

Sakurai H, Takahashi Y, Machida Y (2005) Influence of low-frequency massage device on transdermal absorption of ionic materials. Int J Pharm 305:112–121

Treffel P, Panisset F, Humbert P, Remoussenard O, Bechtel Y, Agache P (1993) Effect of pressure on in vitro percutaneous absorption of caffeine. Acta Derm Venereol 73:200–202